ISOMAse International Society of Ocean, Mechanical and Aerospace Scientists and Engineers

Journal of Ocean, Mechanical and Aerospace
-Science and Engineering-
30th November 2025. Vol.69 No.3

DOI: 10.36842/jomase.v69i3.558

Mechanical Integrity and Weld Characterization of FCAW and GTAW Joints on API 5L CO_2 Fire Suppression Pipes

M Arif Delpero [a], Fardin Hasibuan [a,*], Wendri Putra [b] and Buyung Nul Hakim [a]

[a)]*Program Studi Teknik Mesin, Fakultas Teknik, Universitas Riau Kepulauan, Batam, 29422, Indonesia*
[b)]*PT KTU Shipyard, Batam, Indonesia*

*Corresponding author: fardin.hasibuan123456@gmail.com

Paper History

Received: 11-October-2025
Received in revised form: 19-November-2025
Accepted: 30-November-2025

ABSTRACT

This study investigates the mechanical and macro structural performance of welded joints produced by Flux-Cored Arc Welding (FCAW) and Gas Tungsten Arc Welding (GTAW) on API 5L Grade B low-carbon steel pipes used in marine CO_2 fire suppression systems. The experimental work involved tensile, bending, hardness, and macro structural tests to evaluate the influence of each welding process on joint integrity. Both FCAW and GTAW joints exhibited high mechanical strength, with ultimate tensile strengths of 506MPa and 516MPa, respectively, exceeding the minimum requirement for API 5L Grade B steel. Fracture occurred in the base metal rather than the weld zone, confirming the superior strength and sound fusion quality of the joints. GTAW demonstrated slightly higher tensile performance and cleaner weld morphology due to the controlled heat input and stable arc achieved with 100% argon shielding, whereas FCAW produced marginally higher hardness in the heat-affected zone due to CO_2-induced cooling effects. Macro structural analysis revealed complete penetration and the absence of porosity, slag inclusions, or cracks in both processes. The results comply with AWS D1.1 and ASME Section IX standards, confirming that both welding methods or their hybrid application are suitable for producing safe, reliable, and regulation-compliant marine fire suppression pipelines.

KEYWORDS: *API 5L grade B, Flux-Cored arc welding (FCAW), Gas tungsten arc welding (GTAW), Marine fire suppression systems, Mechanical properties.*

1. INTRODUCTION

Fire suppression systems play a vital role in ensuring safety aboard cargo vessels, where the risk of onboard fires poses a serious threat to human life, cargo, and vessel integrity [1-3]. Among the most widely adopted systems in the maritime industry is the carbon dioxide (CO_2)-based fire suppression system, valued for its effectiveness in extinguishing fires without damaging sensitive equipment or leaving residue[4-6]. These systems rely on a pressurized piping network to rapidly distribute CO_2 to designated compartments during emergencies. Therefore, the mechanical integrity and reliability of these pipelines, particularly at their welded joints, are essential to guaranteeing uninterrupted operation during fire incidents [7-8].

To meet these high-performance demands, API 5L steel pipes are commonly employed in CO_2 suppression systems due to their excellent mechanical strength, corrosion resistance, and conformity with established industry standards [9-12]. The API 5L specification, issued by the American Petroleum Institute, defines stringent requirements for chemical composition, mechanical properties, dimensional accuracy, and non-destructive testing. These pipes are primarily utilized in high-pressure fluid and gas transmission systems and are suitable for both terrestrial and marine applications. However, while API 5L materials are standardized, the performance of welded joints, often the most vulnerable sections of a piping network, depends heavily on the welding process used and the resulting metallurgical characteristics of the joint [13-14].

In the shipbuilding and marine piping industries, two welding processes are predominantly applied: Flux-Cored Arc Welding (FCAW) and Gas Tungsten Arc Welding (GTAW) [15-17]. Each process is selected based on specific technical and operational requirements. FCAW is typically preferred when high productivity and rapid deposition rates are required, particularly in outdoor or high-volume applications involving thick materials [18-20]. It is well-suited for shipyard environments where welding must be completed under strict time constraints and in various positions, including vertical or overhead. FCAW also offers deeper penetration in thicker materials, making it advantageous for large structural joints and heavy-duty components.

Conversely, GTAW is favored for applications demanding precision, weld cleanliness, and superior metallurgical quality. It is widely employed for root passes, thin-wall piping, and safety-critical joints due to its ability to produce defect-free welds with excellent control over arc stability and heat input

[21,22]. Both processes are applied in fabricating marine fire suppression pipelines, where weld quality directly affects system reliability, leak-tightness, and long-term safety. These pipelines operate under high pressure and must withstand harsh marine conditions, including vibration, corrosion, and temperature changes.

Despite the widespread industrial use of FCAW and GTAW, comprehensive comparative studies examining their mechanical and metallurgical performance on API 5L pipes used specifically in shipboard CO_2 suppression systems remain limited. Previous research has largely focused on terrestrial or offshore oil and gas pipelines, often overlooking the unique challenges of marine environments, such as constant vibration, salt exposure, confined spaces, and the strict inspection standards imposed by classification societies.

In practical marine operations, the choice of welding process is also influenced by time and situational constraints. FCAW is commonly applied when repair or installation work must be completed rapidly, particularly during vessel operation, due to its high deposition rate and operational flexibility. In contrast, GTAW is preferred during scheduled maintenance or docking periods when sufficient time is available to prioritize weld quality, precision, and surface finish [23-24]. These differing operational scenarios underscore the importance of evaluating both methods in terms of mechanical integrity, durability, and suitability for marine fire suppression pipelines.

This study aims to address the identified research gap by conducting a comprehensive experimental comparison between Flux-Cored Arc Welding (FCAW) and Gas Tungsten Arc Welding (GTAW) joints on API 5L steel pipes used in carbon dioxide (CO_2)-based fire suppression systems for cargo vessels. The experimental program includes tensile testing, hardness measurement, bend testing, and macrostructural examination, providing a holistic evaluation of weld quality and overall structural performance.

The main scientific contribution of this research is its detailed examination of welding performance in marine CO_2 fire-suppression systems, an essential yet understudied safety application. By experimentally assessing how FCAW and GTAW affect the mechanical integrity, metallurgical characteristics, and compliance of API 5L welded joints with relevant safety standards, this study provides a solid evidence-based framework for selecting and optimizing welding procedures in such systems.

The findings are expected to offer valuable guidance for shipbuilders, welding engineers, and regulatory bodies in improving welding practices and ensuring long-term pipeline reliability. Overall, this work supports the development of safer, more durable, and regulation-compliant CO_2 fire-suppression infrastructure across the maritime industry, reinforcing efforts to enhance vessel safety and reduce operational risks.

2. METHOD

The experimental procedure began with the preparation of API 5L Grade B pipes, which was cut to the required dimensions and beveled to form butt joints with a groove angle between 60° and 70°. Prior to welding, all pipe surfaces were mechanically cleaned using a grinder and wire brush to remove scale, rust, and oil residues, thereby ensuring a clean interface for proper fusion. The pipes were then aligned and secured with tack welds to maintain dimensional stability and minimize joint misalignment during the welding process.

2.1 Material Composition and Mechanical Properties

The experimental material employed in this study is API 5L Grade B carbon steel, which is widely utilized for oil and gas transmission pipelines due to its balance of strength, ductility, and weld-ability. The steel primarily consists of iron (Fe) as the base metal, accompanied by controlled amounts of alloying and residual elements. The typical chemical composition summarized in Table 1 [25].

Table 1: Chemical composition of API 5L Grade B steel

No	Element	Typical Content (weight %)
1	Iron	97.0 – 98.0
2	Manganese	≤ 1.2
3	Carbon	0.26 – 0.28
4	Silicon	≤ 0.40
5	Phosphorus	≤ 0.03
6	Sulfur	≤ 0.03

The mechanical performance of API 5L Grade B complies with the requirements specified in API Specification 5L. The nominal mechanical properties are presented in Table 2 [25].

Table 2: Mechanical properties of API 5L Grade B steel

No	Mechanical property	Typical value
1	Yield Strength	245 MPa
2	Tensile Strength	415 MPa
3	Elongation	23 %
4	Hardness	145 – 150HV

2.2 Flux-Cored Arc Welding (FCAW)

Welding was performed using a Flux-Cored Arc Welding (FCAW) setup equipped with a constant-voltage power source, a flux-cored wire electrode, and a shielding gas consisting of 98% CO_2 supplied at a regulated flow rate of 15–25 L/min. The filler material used in the FCAW process conformed to LB-52U + K-71T specifications, classified as E7016 + E71T according to the AWS standard. All welding parameters—including voltage, current, wire feed speed, and travel speed—were calibrated prior to welding to maintain arc stability and consistent weld quality.

The welding sequence was executed circumferentially along the pipe joint, beginning with the root pass, followed by filling and capping passes to achieve full penetration and adequate reinforcement. The torch was manipulated using a controlled weaving motion to ensure bead uniformity along the pipe circumference, while the electrode angle was dynamically adjusted to accommodate the curvature of the pipe surface. Between each pass, inter-pass cleaning was performed meticulously using a chipping hammer and wire brush to remove slag, thereby minimizing the risk of inclusion and ensuring strong metallurgical bonding between successive layers.

The joints were welded in a butt configuration without back gouging, simulating conditions of restricted root access. The welding progression was performed in a single direction around the pipe, ensuring consistent heat input and uniform penetration. After completion, the welded specimens were allowed to cool naturally under ambient conditions to prevent thermal shock and minimize residual stresses. All residual slag was removed manually, leaving a clean weld surface ready for further inspection and mechanical testing.

The welding parameters used in this study, including current, arc voltage, travel speed, and polarity for each welding pass, are summarized in Table 3.

Table 3: Procedure FCAW

Pass or weld layer (s)	Current		Arc Voltage (V)	Travel speed (mm/min)
	Type & polarity	Amp (A)		
Root pass	Direct Current Electrode Negative (DCEN)	60-75	20-25	50-75
Filler	Direct Current Electrode Positive (DCEP)	110-156	20-25	60-185
Capping	Direct Current Electrode Positive (DCEP)	135-160	20-25	180-230
Capping	Direct Current Electrode Positive (DCEP)	135-160	20-25	180-230

2.3 Gas Tungsten Arc Welding (GTAW)

The Gas Tungsten Arc Welding (GTAW) process was conducted on API 5L pipe prepared in a butt joint configuration. The filler wire used was AWS A5.18, ER70S-6, and 100% argon shielding gas was supplied at a flow rate of 15–25 L/min to protect the weld pool from atmospheric contamination. A 2.4 mm WT20 thoriated tungsten electrode was employed to ensure arc stability and consistent penetration.

The welding sequence followed a multi-pass approach, consisting of a root pass, a hot pass, several filling passes, and a final capping pass. The root pass was deposited with precise control of heat input and arc length to achieve complete fusion at the joint root. A subsequent hot pass was applied to eliminate potential defects such as porosity and to reinforce the root layer. Multiple filling passes were then executed successively to build up weld thickness, improve sidewall fusion, and maintain a controlled heat distribution across the joint. This multi-pass technique also helped reduce distortion by balancing the thermal profile around the pipe circumference.

Finally, a capping pass was performed to produce a smooth weld surface and provide additional mechanical reinforcement. After each pass, inter-pass cleaning was carried out using stainless steel brush to remove surface oxides and other contaminants, ensuring metallurgical continuity between layers.

During welding, the torch was manipulated using a steady forehand technique, allowing precise control of the molten pool and preventing lack of fusion at the groove sidewalls. The travel speed was dynamically adjusted in response to heat accumulation on the pipe surface to prevent excessive penetration or burn-through. The electrode angle was maintained between 70° and 80° relative to the joint line to optimize arc focus and shielding gas effectiveness. Upon completion, all specimens were air-cooled naturally to ambient temperature to minimize distortion and residual stress prior to subsequent testing and evaluation.

The applied welding procedure parameters for all passes are listed in Table 4.

Table 4: Procedure GTAW

Pass or weld layer (s)	Current		Arc Voltage (V)	Travel speed (mm/min)
	Type & Polarity	Amps or wire speed (A)		
1	DCEN	120-128	8-10	60
2	DCEN	120-128	8-10	60
3	DCEN	120-128	8-10	50

3. RESULT

The welding of API 5L pipes using both Flux-Cored Arc Welding (FCAW) and Gas Tungsten Arc Welding (GTAW) processes requires several types of materials, equipment, and supporting tools to ensure optimal weld quality and compliance with established industrial standards. These include consumables such as filler metals and shielding gases, as well as essential welding and inspection instruments. The materials, equipment, and tools used throughout the experimental work are summarized in Table 5,6 and 7.

Table 5: Material sample

No	Material	Specification
1	Base material	API 5L Grade B, diameter pipe : 4 inches, thickness pipe: 8.56 mm
2	Filler (FCAW) Filler (GTAW)	LB-52U + K-71T AWS A5.18

JOMAse | Received: 11-October-2025 | Accepted: 30-November-2025 | [(69) 3: 216-223]
Published by International Society of Ocean, Mechanical and Aerospace Scientists and Engineers, www.isomase.org., ISSN: 2354-7065 & e-ISSN: 2527-6085

Table 6: Equipment specification

No	Equipment	Specification
	FCAW Equipment	
1	Welding Machine (Arc Welding Power Unit)	Manufactured by Daihen Corporation (Japan), the OTC Daihen XD350 SII welding power source operates with a three-phase input voltage of 380/415 V, an input capacity of 18.5 kVA (14.5 kW), and a total unit weight of 121 kg.
2	FCAW Welding Torch	Manufactured by Daihen Corporation (Japan), the 350A welding torch has a rated current capacity of 350 A, supports wire diameters of 0.9, 1.2, and 1.4 mm, and features a gun length of 5 m
3	Wire feeder	Manufactured by Daihen Corporation (Japan), the OTC CM-8202 wire feeder supports wire diameters of 0.9, 1.0, 1.2, 1.4, and 1.6 mm, with an adjustable wire feed speed ranging from 2 to 22 m/min and a total unit weight of 11.5 kg.
	GTAW Equipment	
4	Welding Power Source	Manufactured in Appleton, Wisconsin, USA, the Miller Maxstar 280 welding machine delivers a maximum output current of 280 A, operates on direct current (DC), and has a total unit weight of 21.3 kg.
5	Welding Gas Regulator	Manufactured by Yamato Corporation (Japan), the YR-78 gas regulator has an input pressure range of 0–250 bar, an output pressure range of 0–25 bar, and a total unit weight of 0.5 kg.

Table 7: Tool specification

No	Tool	Specification
1	Tensile Test	Instron Universal Testing Machine, S/N 600DXR9024 model 600DX-C3A-G7F with transverse sample orientation
2	Guided Bend Test	A motor pump bend test machine, serial no: 2906AN19402, model no: A1000PSI/700BAR
3	Hardness Test	The Mitutoyo Vickers Hardness Testing Machine, Model HV-113, S/N:500041203
4	Macro Examination	Optical microscope Nikon Eclipse MA 200

This section presents and analyzes the results obtained from the experimental evaluation of welded joints produced using the Flux-Cored Arc Welding (FCAW) and Gas Tungsten Arc Welding (GTAW) processes on API 5L Grade B steel pipes. The experimental investigation aimed to assess the mechanical performance and integrity of both types of welded joints in order to determine their suitability for CO_2 fire suppression pipeline applications in marine environments.

The evaluation focused on key mechanical properties, including tensile strength, ductility, and hardness, as well as macrostructural examination of the welded joints to verify weld soundness and metallurgical continuity. All testing procedures were conducted under controlled laboratory conditions to ensure accuracy and repeatability. The results are presented in three main parts:

1. Ultimate Tensile and Bending Tests, which assess the overall mechanical strength and ductility of the joints.
2. Hardness Test, which determines the variation in hardness across the weld metal, heat-affected zone (HAZ), and base metal; and
3. Macrostructural Examination, which evaluates weld bead shape, penetration, and potential defect formation.

The findings from these tests provide comprehensive insights into the mechanical behavior and quality of FCAW and GTAW welded joints, serving as a basis for comparing the performance, reliability, and process suitability of the two welding techniques in marine fire suppression pipeline fabrication.

3.1 Ultimate Tensile and Bending Test

Sample tests were conducted on samples containing weld joints and base material for both samples. The tests included tensile testing and bending tests. Results of the ultimate tensile test and bending test of the sample are shown in the following Table 8.

Table 8: Result tensile and bending test

No	Test Criteria	FCAW	GTAW
1		Tensile Test:	
	Ultimate Tensile Strength	506 MPa (location failure base material)	516 MPa (location failure base material)
2		Bending Test:	
	Face Bend	Accepted	Accepted

JOMAse | Received: 11-October-2025 | Accepted: 30-November-2025 | [(69) 3: 216-223]
Published by International Society of Ocean, Mechanical and Aerospace Scientists and Engineers, www.isomase.org., ISSN: 2354-7065 & e-ISSN: 2527-6085

ISOMAse
International Society of Ocean, Mechanical and Aerospace Scientists and Engineers

Journal of Ocean, Mechanical and Aerospace
-Science and Engineering-
30th November 2025. Vol.69 No.3

DOI: 10.36842/jomase.v69i3.558

The tensile test results presented in Table 8 show that both welding processes produced joints with mechanical properties higher than the minimum tensile strength requirement specified for API 5L Grade B steel, which is 415MPa. The FCAW joint achieved an ultimate tensile strength of 506 MPa, while the GTAW joint reached 516MPa, which are approximately 21.9% and 24.3% higher than the standard value of the base material, respectively. These results indicate that the welded joints retained or even enhanced the inherent strength of the parent metal.

In the bending test, both FCAW and GTAW samples were classified as accepted, with no observable cracks or surface discontinuities, further validating the ductile behavior and mechanical integrity of the welded joints. The combined results confirm that both welding processes meet the mechanical criteria required for marine CO_2 fire suppression pipelines, where high structural reliability and safety compliance are critical.

3.2 Hardness Test

Hardness testing was carried out at several points, precisely the base material, HAZ (Heat-Affected Zone), and the weld area. The number of points where hardness was checked totalled 11 points. Figure 1 shows the hardness test points on both samples.

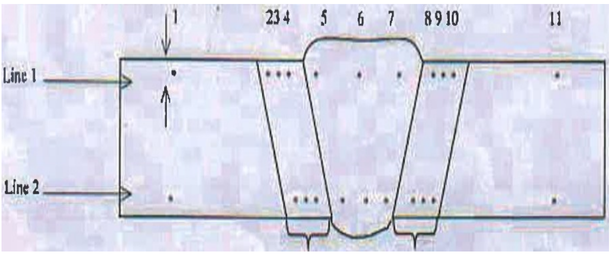

Figure1: Hardness test location

The hardness test was performed using the Vickers Hardness Number (HV) method with an applied test load of 10 kgf. The hardness test results for the material are shown in the Table 9.

Table 9: Result Vickers Hardness Number

Test Location	Vickers Hardness Number (HV) Test Load Applied, 10 kgf			
	FCAW		GTAW	
	Line 1	Line 2	Line 1	Line 2
Base Metal				
1	152	151	152	153
HAZ				
2	184	169	158	186
3	194	178	161	176
4	200	186	162	172
Weld Metal				
5	204	195	213	188
6	211	193	219	180
7	185	193	206	187
HAZ				
8	194	189	164	167
9	187	188	162	163
10	177	185	151	156
Base Metal				
11	147	146	150	153

The hardness test results presented in Table 9 indicate that both the FCAW and GTAW welded joints exhibited hardness values generally higher than those of the API 5L Grade B base material, which typically averages around 150 HV. This comparison highlights the influence of heat input and thermal cycling on the micro structural transformation within the weld metal and heat-affected zones (HAZ).

For the FCAW process, the hardness of the base metal ranged between 146 and 152 HV, closely matching the standard value of API 5L Grade B, confirming that the parent material remained unaffected by thermal degradation. The HAZ displayed elevated hardness levels, varying from 169 to 200 HV, while the weld metal reached its peak between 195 and 211 HV. The hardness value was about 30–40% higher compared to the base metal.

3.3 Macro Examination and Photo

The macro structural examination was conducted to visually assess the quality and soundness of the welded joints produced by both FCAW and GTAW processes. This inspection aimed to identify potential discontinuities such as lack of fusion, porosity, or incomplete penetration that may affect the overall integrity of the weld. The macro photographs presented in Figure 2 illustrate the weld bead geometry, penetration profile, and fusion characteristics observed for each welding process. Based on visual evaluation, both specimens demonstrated acceptable weld morphology and uniform fusion along the joint interface.

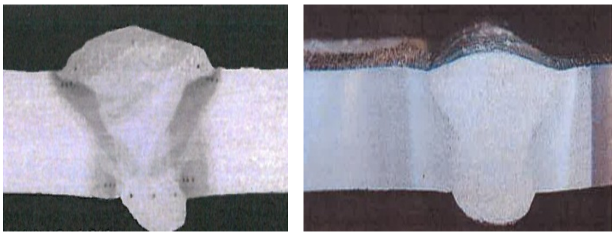

(a) (b)

Figure 2: Macrostructure of weld cross-section (a) FCAW, (b) GTAW

4. DISCUSSION

The results of the mechanical testing show that both FCAW and GTAW welded joints exhibited high mechanical performance, with ultimate tensile strengths (UTS) of 506 MPa and 516 MPa, respectively, and bending test results classified as accepted. Both tensile strength values exceed the minimum requirement for API 5L Grade B steel (≥415 MPa), indicating that the welded joints maintained the original strength of the base material. The fact that fracture occurred in the base metal rather than in the weld zone or HAZ demonstrated the welded joints possessed superior or equivalent strength compared to the parent pipe material. This finding is consistent with the results of Nikulin et.al (2025) [26] and Zhang X & Zheng S (2014) [27], who reported that when optimal parameters are applied, FCAW and GTAW joints can achieve tensile properties comparable to or exceeding the strength of API-grade steels [26-27].

The slightly higher tensile strength achieved by GTAW (516 MPa) compared to FCAW (506 MPa) can be attributed to the controlled heat input, stable arc characteristics, and cleaner

JOMAse | Received: 11-October-2025 | Accepted: 30-November-2025 | [(69) 3: 216-223]
Published by International Society of Ocean, Mechanical and Aerospace Scientists and Engineers, www.isomase.org., ISSN: 2354-7065 & e-ISSN: 2527-6085

fusion achieved through the use of 100% argon shielding gas in GTAW. Nogueira da Silva and Sade (2024) [28] and Rathod (2021) [29] emphasized that the thermal and electrical properties of argon as a shielding gas play a crucial role in maintaining arc stability and uniform heat transfer during the GTAW process [28-29]. Their experimental results demonstrated that the use of 100% argon ensures a cleaner arc column, lower voltage fluctuation, and enhanced ionization, thereby improving the smoothness and fusion quality of the weld pool. GTAW offers excellent arc stability and minimal contamination, which promote uniform grain growth and enhance joint strength. The ER70S-6 filler wire, containing deoxidizers such as manganese (Mn) and silicon (Si), also contributes to improved weld purity and mechanical integrity by reducing oxide inclusions. In contrast, the FCAW process, which uses a CO_2 shielding gas, may promote partial oxidation and slag formation, slightly reducing the efficiency of grain refinement and weld metal homogeneity [30].

Both welding processes passed the face bend test, showing no cracks or surface discontinuities. This confirms the ductile nature and metallurgical soundness of the welded joints, a result in line with findings by Wei P. et al. (2022) [31], who emphasized that successful bend tests signify proper fusion between passes and a uniform distribution of stress across the weld interface [31]. The ductility observed in both FCAW and GTAW joints demonstrates that the multi-pass sequence and adequate inter-pass cleaning performed during the experiment effectively minimized defects such as lack of fusion or slag entrapment, which are critical to ensuring mechanical compliance in pressure piping systems.

The hardness profiles measured across the welded joints revealed that the weld metal region exhibited higher hardness values compared to both the HAZ and the base metal. The maximum hardness recorded for the FCAW process reached 211HV, while the GTAW process showed a peak of 219HV. These values reflect the localized thermal gradients and phase transformations induced during welding. The increase in hardness at the HAZ can be attributed to grain refinement and partial transformation to bainitic or martensitic structures due to rapid cooling in this region, the faster cooling rates near the HAZ in arc welding processes often produce finer microstructures that increase hardness but may reduce toughness slightly[32].

The FCAW process demonstrated a marginally higher hardness in the HAZ compared to GTAW, which can be linked to its higher heat input and faster solidification rates caused by the CO_2-based shielding environment, the CO_2 gas used in FCAW acts as an active shield, promoting higher arc temperatures and increased oxidation rates that lead to the formation of harder microstructures in the fusion boundary. On the other hand, GTAW, using pure argon as the shielding medium, produces a cleaner, more controlled weld pool and promotes softer ferrite–pearlite structures due to a slower cooling rate. This difference explains the slightly lower HAZ hardness observed in the GTAW samples.

Overall, the macro structural examination confirmed sound weld bead geometry, complete penetration, and the absence of visible defects such as porosity, slag inclusions, or cracks in both FCAW and GTAW welded joints. These visual observations validate the mechanical test results, confirming that the multi-pass welding technique and meticulous inter-pass cleaning effectively prevented typical weld discontinuities. A similar level of macro structural integrity has been reported in studies on low-carbon steels, which emphasize that strict adherence to proper welding procedures, together with adequate shielding gas protection, is essential to achieving defect-free welds and ensuring long-term mechanical reliability of welded structure.

Taken together, the experimental findings indicate that both FCAW and GTAW are technically suitable for marine CO_2 fire suppression pipelines, with GTAW offering marginally superior tensile strength and weld cleanliness, while FCAW provides higher deposition efficiency and comparable mechanical strength. These results are consistent with AWS D1.1 and ASME Section IX welding qualification standards, which recognize both processes as appropriate for pressure-containing and structural applications [33-34]. The combination of high strength, acceptable hardness distribution, and defect-free weld morphology confirms that either process, or a hybrid approach using GTAW for root passes and FCAW for fill and cap passes, can be applied effectively to achieve safe, durable, and regulation-compliant welded joints in marine fire suppression systems.

5. CONCLUSION

This study presented an experimental comparison between the Flux-Cored Arc Welding (FCAW) and Gas Tungsten Arc Welding (GTAW) processes for joining API 5L Grade B low-carbon steel pipes used in CO_2 marine suppression systems. The results revealed that both welding techniques successfully produced defect-free joints with high mechanical integrity, as evidenced by ultimate tensile strengths of 506MPa for FCAW and 516MPa for GTAW, both exceeding the minimum requirement for API 5L Grade B steel. The occurrence of fracture in the base metal rather than in the weld region confirmed that the joints possessed strength comparable to or greater than that of the parent material. The superior tensile strength and weld quality of the GTAW joints were attributed to the controlled heat input, arc stability, and cleaner fusion provided by 100% argon shielding gas, which minimized oxidation and promoted uniform metallurgical bonding. Conversely, the slightly higher hardness observed in the heat-affected zone of the FCAW welds was associated with the CO_2-based shielding environment, which induced higher arc temperatures, accelerated cooling rates, and partial transformation to bainitic or martensitic micro structures.

Macro structural evaluation confirmed complete joint penetration, sound bead morphology, and the absence of porosity, slag inclusion, or cracking in both welding processes, validating the effectiveness of the multi-pass sequence and inter-pass cleaning in achieving metallurgical continuity. Collectively, these findings demonstrate that both FCAW and GTAW processes are suitable for pressure-retaining marine applications, with GTAW providing superior weld cleanliness and mechanical uniformity, while FCAW offers higher deposition efficiency and comparable structural performance. Furthermore, the conformity of the experimental results with AWS D1.1 (Clause 6.9) and ASME Section IX (QW-451) standards underscores the reliability and procedural soundness of both welding methods for critical marine safety applications. The weld ments produced by FCAW and GTAW not only satisfied the visual acceptance criteria, being free from cracks, incomplete fusion, and undercut, but also exhibited mechanical

JOMAse | Received: 11-October-2025 | Accepted: 30-November-2025 | [(69) 3: 216-223]
Published by International Society of Ocean, Mechanical and Aerospace Scientists and Engineers, www.isomase.org., ISSN: 2354-7065 & e-ISSN: 2527-6085

properties exceeding the minimum tensile and bend strength requirements prescribed by the ASME qualification standard. This dual compliance confirms that the adopted welding parameters, inter-pass temperature control, and cleaning sequence effectively ensured metallurgical continuity and structural soundness of the API 5L Grade B joints. Overall, the study establishes that either method, or a hybrid sequence employing GTAW for root passes and FCAW for fill and cap passes can be effectively applied to ensure the long-term structural integrity, safety, and regulatory compliance of welded CO_2 marine suppression systems.

REFERENCES

[1] Payri, R., Gimeno, J., Martí-Aldaraví, P., & Carvallo, C. (2020). Parametrical study of the dispersion of an alternative fire suppression agent through a real-size extinguisher system nozzle under realistic aircraft cargo cabin conditions. *Process Safety and Environmental Protection*, 141, 110–122. doi: 10.1016/j.psep.2020.04.022.

[2] Yazir, D. (2022). Application of IF-TOPSIS method on fixed fire fighting systems for cargo hold fires on the dry/bulk cargo ships. *Ocean Engineering*, 260, 111891. doi: 10.1016/j.oceaneng.2022.111891.

[3] Demirboğa, R., & Gül, R. (2003). The effects of expanded perlite aggregate, silica fume and fly ash on the thermal conductivity of lightweight concrete. *Cement and Concrete Research*, 33(5), 723–727. doi: 10.1016/S0008-8846(02)01032-3.

[4] Arvidson, M., & Westlund, Ö. (2024). The development of automatic sprinkler system concepts for maritime vehicle carriers. *Fire Technology*, 60(3), 2125–2153. doi: 10.1007/s10694-024-01563-3.

[5] Aydin, M. (2023). An analysis of human error and reliability in the operation of fixed CO2 systems on cargo ships using HEART Dempster-Shafer evidence theory approach. *Ocean Engineering*, 286, 115686. doi: 10.1016/j.oceaneng.2023.115686.

[6] Moon, H.J., Kim, H.T., & Kim, Y.J. (2013). Design improvement to prevent low-pressure CO2 fire suppression system from plugging up with dry ice. In*International Congress on Advances in Nuclear Power Plants, ICAPP 2013*(pp. 1156–1160). Curran Associates, Inc.

[7] Al-Muslim, H.M., & Arif, A.F.M. (2010). Integrity assessment of multiple dents in oil and gas pipelines using probabilistic design analysis. *Proceedings of the ASME 2010 International Mechanical Engineering Congress and Exposition* (pp. 111–122). American Society of Mechanical Engineers. doi: 10.1115/IMECE2010-37803.

[8] Lv, H., et al. (2023). Data-driven urban gas pipeline integrity detection and evaluation technology system. *Processes*, 11(3), 895. doi: 10.3390/pr11030895.

[9] Sam, S., Kant, N., & Hazra, S.S. (2019). Development of API 5L X70 grade steel through thin slab casting & rolling process. In*ASME 2019 India Oil and Gas Pipeline Conference*. ASME. doi: 10.1115/IOGPC2019-4519.

[10] Zhou, Y., Xie, F., Wang, D., Wang, Y., & Wu, M. (2024). Carbon capture, utilization and storage (CCUS) pipeline steel corrosion failure analysis: A review. Engineering *Failure Analysis*, 155, 107745. doi: 10.1016/j.engfailanal.2023.107745.

[11] Godefroid, L.B., Sena, B.M., & Da Trindade Filho, V.B. (2017). Evaluation of microstructure and mechanical properties of seamless steel pipes API 5L type obtained by different processes of heat treatments. *Materials Research*, 20(2), 514–522. doi: 10.1590/1980-5373-MR-2016-0545.

[12] Zhao, B., Wang, C., Xie, D., & Chen, K. (2018). Research of anti-H2S corrosion seamless line pipe. *Heat Treatment of Metals*, 43(3), 25–29. doi: 10.13251/j.issn.0254-6051.2018.03.006.

[13] Sowards, J.W., Gnäupel-Herold, T., McColskey, J.D., Pereira, V.F., & Ramirez, A.J. (2015). Characterization of mechanical properties, fatigue-crack propagation, and residual stresses in a microalloyed pipeline-steel friction-stir weld. *Materials & Design*, 88, 632–642. doi: 10.1016/j.matdes.2015.09.049.

[14] Simionescu, D., Mitelea, I., Burcă, M., & Uu, I.D. (2018). Mechanical behaviour of narrow gap MAG welding of API 5L X65M steel pipeline. In*IOP Conference Series: Materials Science and Engineering*, 416, 012008. IOPScience. doi: 10.1088/1757-899X/416/1/012008.

[15] Aggarwal, A., Adlakha, D., & Khanna, P. (2023). Development of a mathematical model to predict angular distortion in FCA welded stainless steel 301 plates. In *Materials Today: Proceedings*, 78, 608–613. doi: 10.1016/j.matpr.2022.11.478.

[16] Moisa, R., Popescu, M., & Opris, C. (2011). Problems raised by noxes control at FCAW. In*Annals of DAAAM and Proceedings of the International DAAAM Symposium* (pp. 1265–1266). doi: 10.2507/22nd.daaam.proceedings.617.

[17] Gas tungsten arc welding. (2006). *Welding Journal*, 85(8), 80–82.

[18] Kumar, G.S., Saravanan, S., Balan, A.V., Oscar, J., Ragunath, R., & Ramesh, M. (2020). Influence of FCAW process parameters in super duplex stainless steel claddings. In *Materials Today: Proceedings*, 21, 63–65. doi: 10.1016/j.matpr.2019.05.362.

[19] Malhotra, M., Kashish, Samridhi, & Khanna, P. (2022). Prediction of angular distortion in flux-cored arc welding of stainless steel 301 plates by mathematical modelling. In *Materials Today: Proceedings*, 62, 3681–3688. doi: https://doi.org/10.1016/j.matpr.2022.04.426.

[20] Phillips, S., Quintana, M., Jia, D., Wang, J., & Wang, Y.Y. (2022). Self-shielded flux-cored arc welding - practical approaches for improved performance of girth welds in high-strength steel pipelines. In*Proceedings of the Biennial International Pipeline Conference (IPC)*. ASME. doi: 10.1115/IPC2022-87290.

[21] Singh, G., Dewangan, A.K., Khan, M.F., & Moinuddin, S.Q. (2025). Fundamental review on gas tungsten arc welding of magnesium alloys: Challenges, innovations, and future perspectives. *Welding in the World*, 69(9), 2767–2787. doi: 10.1007/s40194-025-02047-w.

[22] Karhu, M., & Kujanpää, V. (2022). Gas tungsten arc process optimization and assessment for robotized position welding of austenitic stainless steel edge joints. *CIRP Journal of Manufacturing Science and Technology*, 36, 12–22. doi: 10.1016/j.cirpj.2021.10.012.

[23] von Querfurth, B., et al. (2025). AI-driven autonomous adaptative feedback welding machine. *Welding in the*

World, 69(5), 1419–1426. doi: 10.1007/s40194-024-01898-z.

[24] Rathod, D.W. (2021). Comprehensive analysis of gas tungsten arc welding technique for Ni-base weld overlay. In*Advanced welding and deforming* (pp. 105–126). Elsevier. doi: 10.1016/B978-0-12-822049-8.00004-9.

[25] PT Steel Pipe Industry of Indonesia Tbk. (n.d.). API 5L grade B material characteristics you must know. https://www.spindo.com/api-5l-grade-b-material-characteristics-you-must-know.

[26] Nikulin, S.A., Rogachev, S.O., Belov, V.A., Turilina, V.Y., & Shplis, N.V. (2025). Effect of high temperature on the strength of the base metal and the weld metal in a welded joint of low-carbon steels. *Russian Metallurgy (Metally)*, 2025(3), 632–637. doi: 10.1134/S003602952570020X.

[27] Zhang, X.A., & Zheng, S.L. (2014). Experimental study in fracture and fatigue property of weld jointing with thick Q345R steel plan. *Petrochemical Equipment*, 43(1), 17–22.

[28] da Silva, N.N., & Sade, W. (2024). The effects of preheating the shielding gas used in gas tungsten arc welding. *Welding Journal*, 103(10), 298–307. doi: 10.29391/2024.103.026.

[29] Rathod, D.W. (2021). Comprehensive analysis of gas tungsten arc welding technique for Ni-base weld overlay. In*Advanced welding and deforming* (pp. 105–126). Elsevier. doi: 10.1016/B978-0-12-822049-8.00004-9.

[30] Aggarwal, S., Dwivedi, M., & Khanna, P. (2022). Mathematical modelling to predict the dilution in FCA welded low carbon steel plates. In *Materials Today: Proceedings*, 56, 3512–3519. doi: 10.1016/j.matpr.2021.11.226.

[31] Wei, P., Wu, M., Liu, D., Liang, Y., & Zhao, Z. (2022). Face bend property of 7N01-T4 aluminum alloy MIG welded joint by using different welding wires. *Metals*, 12(5), 873. doi: 10.3390/met12050873.

[32] Guo, A., Misra, R.D.K., Liu, J., Chen, L., He, X., & Jansto, S.J. (2010). An analysis of the microstructure of the heat-affected zone of an ultra-low carbon and niobium-bearing acicular ferrite steel using EBSD and its relationship to mechanical properties. *Materials Science and Engineering: A*, 527(23), 6440–6448. doi: 10.1016/j.msea.2010.06.092.

[33] ASME. (2025). 2025 ASME Boiler and Pressure Vessel Code, Section IX: Qualification standard for welding, brazing, and fusing procedures; welders; brazers; and welding, brazing, and fusing operators. American Society of Mechanical Engineers. Available: www.asme.org/cer

[34] American Welding Society. (2020). Structural welding code-steel (AWS D1.1/D1.1M:2020). American Welding Society.